JOURNAL OF CATALYSIS 142, 617–629 (1993)

The Structure and Activity of Silica-Supported Palladium–Cobalt Alloys

I. Alloy Homogeneity, Surface Composition, and Activity for Neopentane Conversion

W. JUSZCZYK,* Z. KARPIŃSKI,* D. ŁOMOT,* J. PIELASZEK,*,[1] Z. PAÁL,† AND A. YU. STAKHEEV‡

*Institute of Physical Chemistry of the Polish Academy of Sciences, ul. Kasprzaka 44/52, 01-224 Warsaw, Poland; †Institute of Isotopes of the Hungarian Academy of Sciences, P.O. Box 77, H-1525 Budapest, Hungary; and ‡N. D. Zelinsky Institute of Organic Chemistry of the Russian Academy of Sciences, 47 Leninskii Prospekt, Moscow 117913, Russia

Received September 7, 1992; revised January 11, 1993

Chemisorption of H_2 and CO, temperature-programmed reduction (TPR), X-ray diffraction (XRD), X-ray photoelectron spectroscopy (XPS), and neopentane conversion show that differences in preparation method and overall metal loading lead to the formation of different Pd–Co bimetallic materials (changes in reducibility, metal particle size, and lateral homogeneity). Well-homogenized Pd–Co particles exhibit a very pronounced minimum in the plot of catalytic activity versus Pd–Co alloy composition. At the same time, a maximum exists in the isomerization selectivity vs the alloy composition. These deviations from the catalytic behavior of physical mixtures of the monometallic (Pd and Co) catalysts provide a basis for the estimation of how two metals interact with each other in a supported catalyst. Incipient wetness impregnation of silica by considerable amounts (10 wt%) of metal salts leads to the formation of catalyst precursors which are fully reduced at 380°C yielding good dispersion and lateral homogeneity. Chemisorption and *in situ* XRD studies are compatible with the kinetic investigations, but information on metal interaction by these methods is less clear. For high metal-loaded Pd–Co/SiO_2 catalysts, comparison of H_2 chemisorption and XRD data suggests surface enrichment in palladium, which is confirmed by XPS.

INTRODUCTION

A wide interest in bimetallic systems in catalytic research and industrial processes was motivated by the technological superiority (better stability and/or selectivity) of many alloy catalysts in naphtha reforming. Preparation leading to the formation of a well-homogenized bimetallic system and its characterization in the case of highly dispersed, low-loaded bimetal/support catalysts still present very real difficulties (*1*). Considerable progress in utilizing physical methods (e.g., extended X-ray absorption fine structure spectroscopy (EXAFS), X-ray photoelectron spectroscopy (XPS), X-ray diffraction (XRD)) to investigate the very complex surfaces of bimetals dispersed over carriers has recently been achieved. However, it should be stressed that quite frequently the use of these sophisticated techniques may bring ambiguous results, due to problems associated with insufficient sensitivity or uncertain interpretation (e.g., chemical shifts in XPS), and because conditions of measurements are so different from those of catalytic reactions. This is the reason why chemical probing of catalysts is still so essential.

We turned our attention to supported Pd–Co alloy catalysts for two reasons. First, having some experience with characterization of supported monometallic palladium catalysts using various catalytic probes (*2–4*), we wished to extend our

[1] To whom correspondence should be addressed.

0021-9517/93 $5.00

"chemical" approach to probe more complex objects such as the surfaces of supported Pd-based alloys. Second, the choice of cobalt as an additive to palladium seemed attractive because the both metals exhibit quite different chemical properties (e.g., reducibility) and, in particular, catalytic properties. Interaction of cobalt with alkanes leads almost exclusively to their hydrogenolysis (*5*, *6*), whereas isomerization, in addition to hydrogenolysis, is usually observed on palladium (*2*, *3*, *5*, *7*).

We studied two series of silica-supported Pd–Co catalysts prepared by impregnation. We were aware that coimpregnation of silica with an aqueous solution of two metal salts may not lead to preparation of well-homogenized, highly dispersed bimetallic catalysts. Several attempts to improve alloy preparation techniques should be mentioned here. One of them involves the use of intermetallic compounds, such as mixed carbonyl clusters of rhodium and cobalt (*8*). Another method, called "controlled surface reaction," elaborated by Margitfalvi *et al.* (*9*), leads to the deposition of one metal over another. When either of these methods is employed, one would expect a better interaction of two alloy components than in the case of random deposition of metals in carrier pores during impregnation and drying. Optimizing the preparation method was, however, outside the scope of the present work which was aimed at evaluating methods to diagnose whether two highly dispersed metals interact with each other on a support. For this reason we used two different impregnation procedures to obtain two series of Pd–Co/SiO_2 catalysts characterized by different alloy homogeneity. The first series consisted of 10 wt% metal samples, prepared by incipient wetness impregnation with careful rotary agitation during all stages of the preparation. This method should result in deposition of material inside carrier pores. For comparison, another series was prepared from solution with excess solvent, without any mixing. A low metal loading of only 1 wt% was used in this series which further lowers the chance of forming mixed metals as the metal phases cover only a tiny fraction of the carrier surface (specific surface area of 300 m^2/g).

Our intention was to investigate these two series of silica-supported Pd–Co alloys by using catalytic probes and to verify the deductions by physical methods. The use of such a combination should lead to more convincing conclusions. Preliminary results have recently been reported as a short communication (*10*). This paper deals with characterization of the silica-supported Pd–Co alloys by using neopentane conversion as a catalytic probe alongside other physical and chemical methods. Part II of this series will report studies on the catalytic conversion of *n*-hexane and methylcyclopentane (*11*).

EXPERIMENTAL METHODS

Catalyst Preparation and Pretreatment

Two series of silica-supported Pd–Co alloys were prepared by coimpregnation of an aqueous solution of $PdCl_2$ and $CoCl_2$ with a Serva silica support (puriss, 80–100 mesh). The first series, of 10 wt% metal loading, was prepared by incipient wetness coimpregnation with a solution of the pure metals (specpure wires from Johnson–Matthey) in hydrochloric acid. During impregnation and drying with infrared lamps a good mixing was assured by a rotary motion of a beaker containing the catalyst precursor components. The second series of catalysts (of 1 wt% metal loading) was intentionally "poorly" prepared: impregnation was carried out from a slurry of Pd, Co chlorides (analytical grade, from POCh, Gliwice, Poland) in doubly distilled water, *without any stirring*. After removing excess water, it was easy to notice a gradient of color along the length of the impregnated solids suggesting very poor mixing of the two metal salt components. Catalysts are designated Pd*X*Co*Y*, where *X* is the atom % Pd and *Y* the atom % Co.

After impregnation, the catalysts were dried in an air oven at 120°C for 8 h. Then they were precalcined in an air flow, in a

fluidized bed reactor, ramping the temperature from room temperature (RT) up to 450°C at 3°C/min, and kept at 450°C for 3 h. After calcination the catalysts were transferred to glass-stoppered bottles, and were stored in a desiccator.

Before kinetic, chemisorption, XPS, and XRD experiments each sample was calcined in an O_2 flow at 300°C for 30 min, flushed with Ar (or He) at 300°C for 5–10 min, and, finally, reduced in H_2 ramping the temperature from RT up to 380°C, and kept at this temperature for 15 (or 2) h. All gases, except oxygen, were purified by passing through drying traps with final purification over MnO/SiO_2. Carbon monoxide was 99.995% pure (Van Eeghen, The Netherlands).

Chemisorption and Temperature-Programmed Reduction (TPR)

The chemisorption of hydrogen and CO was measured in a static volumetric apparatus equipped with a high-vacuum system and a Setra pressure transducer (Model 204D). In order to avoid β-hydride formation (in the case of Pd, (*12*)) as well as to increase rate of adsorption (for Co-containing samples, (*13*)), the H_2 chemisorption measurements were performed at 100°C. Amounts of irreversibly chemisorbed hydrogen, estimated from hydrogen desorption isotherm by a back-extrapolation method, constituted the basis for calculating metal dispersions (assuming $H/M_s = 1$).

TPR experiments were carried out in a flow of 6% H_2/Ar (35 ml/min) through a catalyst bed with an 8°C/min temperature ramp. Difference TPR spectra, after reduction in H_2 at 380°C, were also recorded (only for 10 wt% series). In these experiments, prereduced catalysts were purged and cooled down in argon and studied by TPR up to 850°C. A standard GowMac katharometer cell was used.

Neopentane Conversion

The reaction of neopentane (Merck) with hydrogen was investigated in a static circulation system in the manner described previously (*3*). The catalyst (0.05–0.5 g) was deposited in a U-tube fitted with a fritted disc and thermocouple well. After calcination and reduction the temperature was lowered to a desired reaction temperature. The whole system was made of glass with Young stopcocks and $\frac{1}{4}$" Cajon Ultra-Torr fittings for connecting the reactor. The composition of the reaction mixture (neopentane + hydrogen) was measured by a Barocel Electronic Manometer (Model 1174). The alkane partial pressure was always kept at 10 Torr (1 Torr = 133.3 Pa). The ratio of hydrogen-to-alkane was 10 : 1. The reaction was followed by gas chromatography (HP 5890 Series II with FID, 6-m squalane/Chromosorb P column, with a HP 3396 Series II integrator).

Turnover frequencies (TOFs) were calculated on the basis of the dispersion measured by H_2 chemisorption. Initial product distributions (= selectivities) were calculated as the carbon percentage of neopentane consumed in the formation of a designated product; for example, the mol% of methane from neopentane would be divided by 5 and normalized in deriving the product distribution.

X-Ray Diffraction (XRD) and X-Ray Photoelectron Spectroscopy (XPS)

XRD experiments were performed on a standard Rigaku-Denki diffractometer using CuK_α radiation. An X-ray diffraction camera-gradientless reactor (*14*) was used for measurements in a controlled atmosphere. After reduction at 380°C for 15 h, Pd–Co/SiO_2 samples were scanned in the 2θ range of 30 to 72°. The data were collected by a step-by-step technique. The resulting diffraction profiles originating from the metal phase were obtained by the method of subtraction of the support background profile (*15*) with appropriate data smoothing (*16*).

XPS experiments were performed on a VG ESCALAB-5 spectrometer using unmonochromatized Al$K_{\alpha 1,2}$ radiation. The spectrometer was equipped with a high pressure cell permitting sample pretreatment to be carried out in various atmospheres and

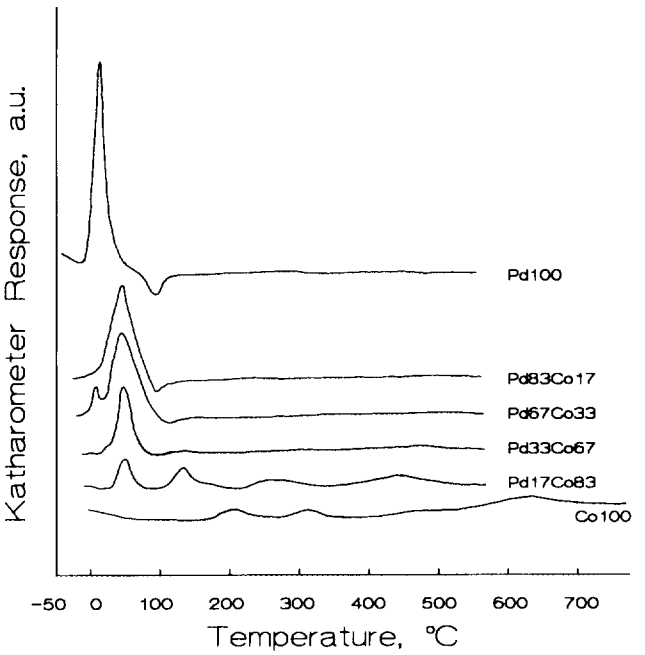

FIG. 1. TPR profiles for 1 wt% Pd–Co/SiO_2 catalysts. In designation of catalysts, PdXCoY means X – atom % Pd, Y – atom % Co.

at elevated temperature. Samples for XPS studies were pressed in a hydraulic die to form thin, smooth pellets, and placed in the high pressure cell. After reduction in flowing H_2 at 380°C for 2 h, the samples were transferred to the analytical chamber of the spectrometer without contact with air. The surface Pd/Co atomic ratio was estimated from the integral intensities of Pd 3*d* and Co $2p_{3/2}$ lines using the Wagner sensitivity factors (*17*). A linear background was subtracted before peak integration.

RESULTS

Temperature-Programmed Reduction (TPR)

Figures 1 and 2 show TPR profiles of 1 and 10 wt% Pd–Co/SiO_2 catalysts, respectively. The reducibility of 1 wt% Co/SiO_2 catalyst was found to be low: up to ca. 500°C only 6% of the cobalt is reduced. Above 500°C, a diffuse TPR peak starts to appear, but reduction is not completed at 800°C. The TPR spectrum of the 1 wt% Pd/SiO_2 catalyst shows one peak near 0°C (100% reduction) but the end of its tail is deformed by a negative peak showing hydrogen evolution from decomposition of the β-PdH phase. Figure 1 shows that the TPR profiles for all bimetallic catalysts, excluding Pd17Co83, likewise exhibit single peaks. However, their maxima are shifted towards higher temperatures, by ca. 40°C, with respect to the 1 wt% Pd/SiO_2. This fact may be indicative of some influence of cobalt. Another fact, namely the presence of a negative peak ascribed to H_2 evolution from β-hydride decomposition suggests that, as opposed to the previous observation, at the stage of TPR, both alloy components are rather separated. Hydrogen solubility in Pd–Co alloys with Co content $\geq$ 10 at% is very low (*18*); therefore for well-mixed Pd–Co alloys one should not expect any formation of a β-hydride phase in the stream of 6% H_2/Ar. In spite of this, the negative peak on the tail of the principal TPR peak appeared for Pd67Co33 and

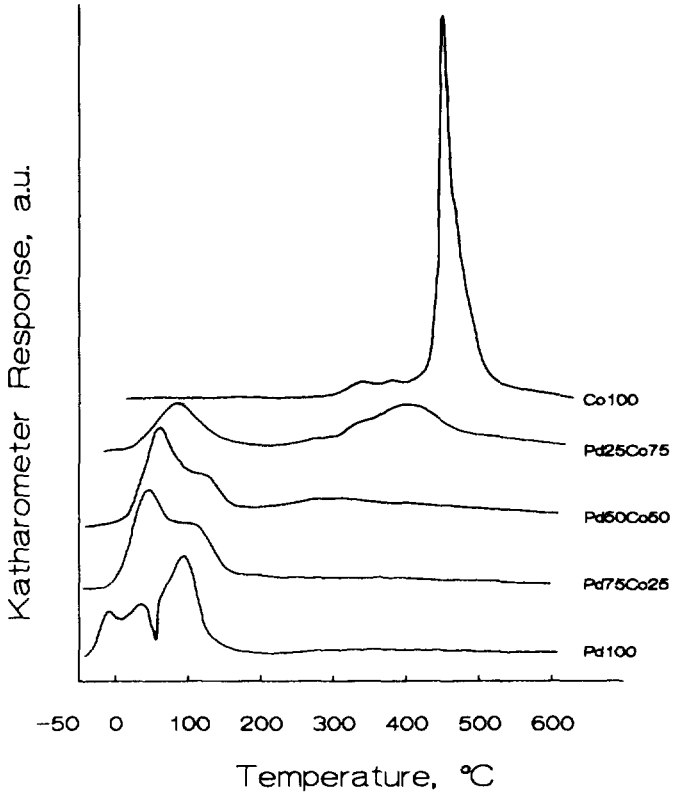

FIG. 2. TPR profiles for 10 wt% Pd–Co/SiO_2 catalysts (designation of catalysts as in Fig. 1).

Pd33Co67 samples (Fig. 1). In addition, integration of the TPR peak areas gave results which may suggest that only palladium is reduced. Assuming that the error in the TPR integration is ca. ±5%, we cannot exclude reduction of small amounts of cobalt, especially when the TPR peak shifted with cobalt content to higher temperatures. An exception mentioned above was the TPR spectrum of the Pd17Co83/SiO_2 where four peaks were seen between 0 and 500°C. One of these, at 45°C, is probably due to reduction of almost pure palladium; the others are believed to be characteristic for reduction of Pd–Co mixed systems.

TPR results for 10 wt% Pd–Co/SiO_2 catalysts showed that the silica-supported Pd and Pd–Co bimetallics are fully reduced below 380°C, but the 10 wt% Co/SiO_2 sample exhibits a hydrogen consumption maximum at ca. 450°C (Fig. 2). The peculiar shape of the TPR profile of Pd100 indicates the reduction of three types of species and decomposition of the β-PdH phase. No peak corresponding to decomposition of β-PdH was seen on the bimetallic samples. Moreover, TPR peaks of 10 wt%-loaded alloy catalysts were shifted towards higher temperatures as compared to the positions of analogous TPR peaks of the low-loaded Pd–Co/SiO_2 samples. The sample with highest Co content (Pd25Co75) displayed only one high-temperature peak at 400°C as opposed to two peaks with 1 wt% Pd17Co83/SiO_2.

Difference TPR spectra of all 10 wt% metal-loaded samples recorded after reduction in H_2 at 380°C (for 2 or 15 h) showed no further reduction. This means that a prolonged hydrogen treatment at 380°C leads to complete reduction.

TABLE 1

Chemisorption and XRD Data of Pd–Co/SiO_2 Catalysts

Nominal composition		Metal dispersion		Metal particle size[b] (nm) (from D_H)	XRD analysis	
at% Pd	at% Co	D_H	D_{CO}		Phase composition	Particle size (nm)
			1 wt% Pd–Co/SiO_2			
100	—	0.22_1	—[a]	5.1	fcc, 100%Pd	6.8 (111) 6.0 (200)
83	17	0.19_4	—[a]	4.9[c]	*d*	—
67	33	0.15_2	—[a]	5.3[c]	*d*	—
50	50	0.11_3	—[a]	5.7[c]	*d*	—
33	67	0.10_5	—[a]	4.3[c]	*d*	—
17	83	0.06_4	—[a]	4.8[c]	*d*	—
—	100	0.02_9	—[a]	—	Not detected	—
			10 wt% PdCo/SiO_2			
100	—	0.50	0.44	2.2	fcc, 100%Pd	2.2
75	25	0.44	0.44	2.3	fcc, 31%Co	<2
50	50	0.27	0.30	3.7	fcc, 62%Co	<2
25	75	0.11	0.20	8.0	*hcp(Co)* + some fcc (PdCo)	4.0
—	100	0.10	0.07	9.0	*hcp (Co)* + fcc(Co)	8.1

[a] Not measured.

[b] Metal particle size from chemisorption (H/M, where M = Pd + Co), assuming spherical particles, for Pd: $d_{Pd} = 1.12/(H/Pd)$, according to Ichikawa *et al.* (*19*); for Co: $d_{Co} = 0.9/(H/Co)$. In order to acknowledge some contribution of Co (hcp), the factor 0.9 in the latter formula is somewhat lower than the value (0.96) used by Reuel and Bartholomew (*13*) for supported Co (fcc). For 10 wt% Pd–Co bimetallics, respective factors were taken as proportional to nominal compositions.

[c] Particle size of palladium in 1 wt% Pd–Co/SiO_2 catalysts is

$$d_{Pd}(\text{nm}) = \frac{1.12 \cdot x_{Pd}}{[H/(Pd + Co) - x_{Co} \cdot (H/Co)]},$$

where $H/Co = 0.02_9$, as for 100 at% Co/SiO_2.

[d] Only 100% (or almost nearly 100%) Pd(111) reflections were well seen. The intensity of the Pd(111) peak monotonously increased with Pd content. An asymmetric shape of the peak would suggest some presence of Pd–Co phase(s). The presence of the Co hcp phase was rather speculative.

Chemisorption of H_2 and CO, and X-Ray Diffraction Results

Table 1 shows chemisorption data for 1 and 10 wt% Pd–Co/SiO_2 catalysts, respectively. Metal dispersions, H/M, based on a 1 : 1 adsorption stoichiometry, are also converted to yield metal particle sizes. The subsequent values are compared with particle sizes resulted from X-ray diffraction line broadening. A reasonable agreement is exclusively noticed in the case of monometallic, 10 wt% Pd/SiO_2 and 10 wt% Co/SiO_2 samples.

The last column in Table 1 presents results of phase analysis by XRD. The Pd–Co alloy composition was calculated from the position of the fcc(111) Pd–Co diffraction peak.

Figure 3 displays a relationship between H/M and atom % cobalt for 1 wt% Pd–Co/SiO_2 and 10 wt% Pd–Co/SiO_2. A good linear correlation is seen in the case of the low-loaded series. We think that this is another indication of a rather weak interaction between two metals. Accordingly, in the case of the low-metal loaded series, we calcu-

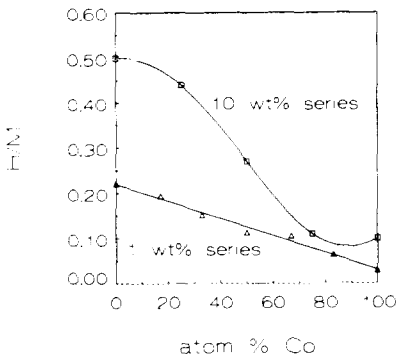

FIG. 3. Hydrogen chemisorption data (H/M, where M = Pd + Co) for 1 wt% Pd–Co/SiO_2 (triangles) and 10 wt% Pd–Co/SiO_2 (squares) catalysts.

lated the particle size of palladium assuming additivity of individual chemisorption contributions from both components (Table 1, for 1 wt% Pd–Co/SiO_2). In the case of 10 wt% Pd–Co/SiO_2, an attempt to use a linear correlation produced a much worse fit than in the case of the low-loaded series (Fig. 3).

Table 2 presents Pd/Co atomic ratios obtained by XPS for 10 wt% Pd-Co/SiO_2 catalysts after reduction in H_2 at 380°C for 2 h. The XPS Pd/Co atomic ratios are higher than bulk values.

Neopentane Conversion

The reaction of neopentane with hydrogen on Pd–Co/SiO_2 catalysts was examined in the temperature range of 230–280°C.

TABLE 2

Pd/Co Atomic Ratios Obtained by XPS as Compared to the Bulk Values

Nominal composition		$(Pd/Co)_{bulk}$[a]	$(Pd/Co)_{surface}$[b]
at% Pd	at% Co		
75	25	3.00	5.55
50	50	1.00	1.92
25	75	0.33	0.79

[a] From nominal composition.

[b] From the integral intensities of Pd 3*d* and Co $2p_{3/2}$ lines using the Wagner sensitivity factors (*17*).

Turnover frequencies and initial product distributions (= selectivities) are presented in Table 3 (for 1 wt% Pd–Co/SiO_2) and Table 4 (for 10 wt% Pd–Co/SiO_2). Both 1 wt% as well as 10 wt% Co/SiO_2 catalysts exhibit only hydrogenolysis activity (no trace of isomerization).

Turnover frequencies at 240°C for 1 and 10 wt%-loaded catalysts are shown in Fig. 4 as a function of Pd–Co alloy composition. Experimental data for a 1 : 1 physical mixture of two monometallic catalysts are also included. It is seen that the catalytic activity of the Pd–Co alloys passes through a minimum. A similar picture was obtained at higher reaction temperatures.

Isomerization selectivities of two series of catalysts are presented in Fig. 5. For 10 wt%-loaded series, Pd–Co alloys display much higher selectivity than Pd/SiO_2.

Figure 6 shows changes of the fragmentation factor, ζ, with Pd–Co alloy composition. The fragmentation factor characterizes the depth of hydrogenolysis, as the number of fragment molecules per molecule of hydrocarbon hydrogenolyzed (*20*). A common course is seen for the both series of Pd–Co catalysts. One experimental point for the 1 : 1 physical mixture of 10 wt% Pd/SiO_2 + 10 wt% Co/SiO_2 lies only slightly below the curve for two series of Pd–Co alloy catalysts.

DISCUSSION

As mentioned in the Introduction, our intention was to find useful methods for characterization of highly dispersed bimetallic Pd–Co catalysts, and in particular to estimate the degree of interaction between the two metals as well as the surface composition of the alloy phase. Preparation of two different series of Pd–Co catalysts has helped us to assess the diagnostic power of various physical and catalytic probes, as we hope to make clear in the following subsections.

TPR and Chemisorption on Pd–Co/SiO_2

Figure 2 demonstrates that reduction of all 10 wt% Pd–Co/SiO_2, except Co100, is

TABLE 3

Neopentane Conversion over 1 wt% Pd–Co/SiO_2: Turnover Frequencies and Initial Product Distributions

Catalyst		Reaction temp. (°C)	Initial product distribution (%)[a]					Turnover frequency (1/s)
at% Pd	at% Co		Me	Et	Pr	iB	iP + nP	
100	—	241	11.4	0.4	1.2	35.8	51.1	9.68×10^{-6}
		251	13.0	0.2	1.0	44.9	40.9	2.71×10^{-5}
		263	16.1	0.1	1.4	51.5	30.8	8.94×10^{-5}
83	17	243	12.2	1.1	1.7	32.1	52.9	5.15×10^{-6}
		253	11.1	0.2	0.8	37.0	51.0	1.30×10^{-5}
		264	11.7	0.1	0.6	41.1	46.5	4.21×10^{-5}
67	33	242	16.5	2.7	4.5	27.8	48.5	1.91×10^{-6}
		254	14.4	0.4	1.5	29.8	53.9	4.47×10^{-6}
		264	12.4	0.7	1.0	37.0	49.0	1.03×10^{-5}
50	50	241	12.9	4.2	3.1	23.9	55.9	2.18×10^{-6}
		252	21.6	2.4	5.7	29.3	41.1	2.33×10^{-6}
		265	21.7	1.8	3.0	32.8	40.7	5.10×10^{-6}
33	67	241	23.4	4.5	7.2	41.1	23.7	2.04×10^{-6}
		253	30.3	2.6	5.1	42.3	19.8	3.15×10^{-6}
		267	41.1	3.7	5.6	34.6	15.0	7.50×10^{-6}
17	83	241	37.1	6.3	6.6	50.1	—	5.91×10^{-6}
		251	43.7	4.2	7.0	40.6	4.5	1.19×10^{-5}
		261	53.2	4.4	7.7	32.0	2.6	2.18×10^{-5}
—	100	240	72.1	10.5	10.2	7.2	—	3.33×10^{-5}
		251	82.3	6.1	5.7	6.0	—	3.25×10^{-5}
		262	89.5	4.1	2.8	3.6	—	6.01×10^{-5}

[a] Me = methane, Et = ethane, Pr = propane, iB = isobutane, iP = isopentane, and nP = *n*-pentane.

TABLE 4

Neopentane Conversion over 10 wt% Pd–Co/SiO_2: Turnover Frequencies and Initial Product Distributions

Catalyst		Reaction temp. (°C)	Initial product distribution (%)[a]					Turnover frequency (1/s)
at% Pd	at% Co		Me	Et	Pr	iB	iP + nP	
100	—	240	10.7	0.1	0.3	32.8	56.9	1.06×10^{-5}
		251	12.7	0.2	0.8	40.8	45.5	3.23×10^{-5}
		263	17.6	0.4	2.5	48.1	31.4	9.63×10^{-5}
75	25	239	6.2	—	0.5	19.3	73.9	2.22×10^{-6}
		251	8.4	0.2	0.5	26.6	64.3	7.27×10^{-6}
		263	13.2	0.3	1.2	37.5	47.8	2.43×10^{-5}
50	50	242	10.8	2.6	6.0	14.9	65.7	1.74×10^{-7}
		252	10.3	1.0	0.3	24.0	64.4	3.55×10^{-7}
		265	8.3	0.6	1.2	21.2	68.7	1.05×10^{-6}
25	75	242	8.6	7.1	10.1	14.1	60.1	1.39×10^{-7}
		251	12.0	1.6	3.2	18.6	64.5	2.71×10^{-7}
		263	11.6	4.0	2.5	19.1	62.8	7.77×10^{-7}
—	100	240	88.3	4.9	2.3	4.5	—	1.13×10^{-6}
		257	89.8	4.5	3.1	2.6	—	2.90×10^{-6}
		271	96.0	2.1	0.8	1.1	—	6.10×10^{-6}

[a] As in Table 3.

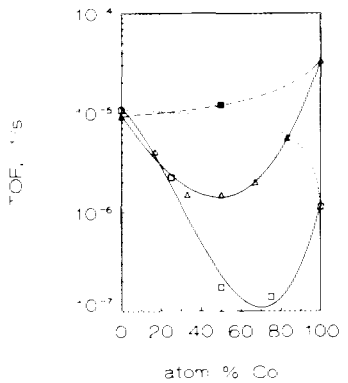

FIG. 4. Turnover frequency for neopentane conversion vs the Co bulk content for 1 wt% (triangles) and 10 wt% Pd–Co/SiO_2 (open squares), and a physical mixture of 10 wt% Pd/SiO_2 + 10 wt% Co/SiO_2 (ratio = 1 : 1) (filled square) catalysts at 240°C. Also shown are hypothetical dependences of TOF for physical mixtures of 1 wt% Pd/SiO_2 + 1 wt% Co/SiO_2 (dashed line) and for physical mixtures of 10 wt% Pd/SiO_2 + 10 wt% Co/SiO_2 (dotted line).

virtually complete at 380°C. Although the pure cobalt catalyst exhibits its TPR peak at 450°C, a featureless difference TPR line of this catalyst (not shown) indicates that reduction at 380°C for 15 (or 2) h is complete.

On the basis of TPR lines obtained for bimetallic catalysts it is difficult to assess whether one deals with well mixed metal components at the stage of TPR. That is why we decided to run our catalysts after prolonged, 15 h, reduction at 380°C. Such a severe pretreatment should facilitate interdiffusion of both metal components.

On the other hand, 1 wt% metal-loaded catalysts exhibit quite different TPR characteristics (Fig. 1). First, cobalt is only partly reduced at temperatures below 800°C. This is not surprising, because similar observations for low metal loaded Co catalysts were already reported (*13, 21*). Second, relatively low intensities of TPR lines suggest that, within experimental error (±5%), only very small amounts of cobalt are reduced, in addition to an entire reduction of palladium.

Thus we believe that, accepting certain difficulties in assessing TPR spectra, in the series of 10 wt% metal-loaded catalysts, the Pd–Co alloy phase is better homogenized than in the 1 wt% metal-loaded samples. An additional fact is that the negative peaks in Figs. 1 and 2, indicative of β-PdH decomposition, are seen only for 1 wt% Pd–Co/SiO_2 catalysts, where palladium does not seem to interact strongly with cobalt.

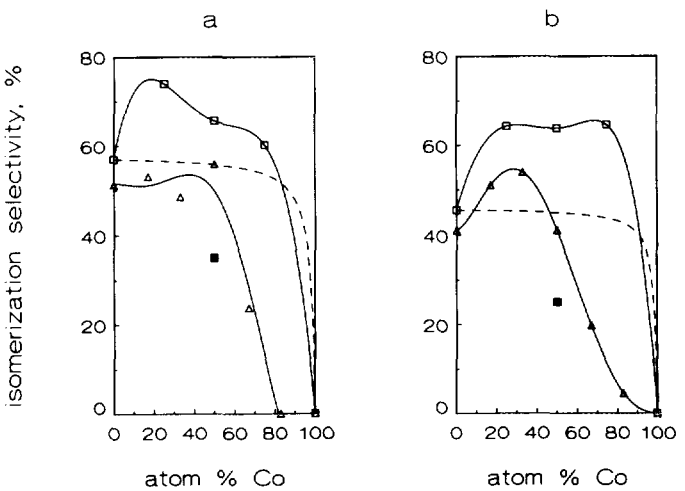

FIG. 5. Isomerization selectivity vs the Co bulk content for 10 wt% Pd–Co/SiO_2 (open squares), 1 wt% Pd–Co/SiO_2 (triangles) catalysts, and a physical mixture of 10 wt% Pd/SiO_2 + 10 wt% Co/SiO_2 (ratio = 1 : 1) (filled square): (a) at 240°C and (b) at 250°C. Dashed lines represent hypothetical curves for physical mixtures of 10 wt% Pd/SiO_2 and 10 wt% Co/SiO_2 catalysts.

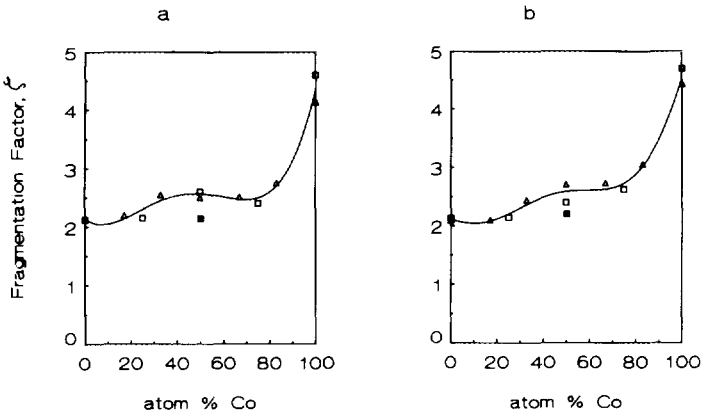

FIG. 6. Fragmentation factor, ζ (see text), vs the Co bulk content for 10 wt% Pd–Co/SiO_2 (open squares), 1 wt% Pd–Co/SiO_2 (triangles) catalysts, and a physical mixture of 10 wt% Pd/SiO_2 + 10 wt% Co/SiO_2 (ratio = 1 : 1) (filled square): (a) at 240°C and (b) at 250°C.

Uptakes of chemisorbed H_2 on 1 wt% Pd–Co/SiO_2 samples (Table 1) were rather low as compared to corresponding values for 10 wt%-loaded samples. In addition, the H/M values decreased linearly with increase of cobalt content (Fig. 3). This fact may suggest (but it is not a definite proof of) a situation where palladium interacts only very weakly with cobalt. We shall return later to this problem.

XRD and XPS

Table 1 shows that for three 10 wt% bimetallic catalysts, XRD line broadening implies higher metal dispersions than the respective values from H_2 chemisorption. However, in the case of pure Pd and Co samples, both methods give good agreement. In addition, lattice parameters of Pd–Co alloys indicate the presence of phases with a palladium deficit, compared to nominal compositions of 10 wt% Pd–Co/SiO_2 catalysts. We conclude that the enormously broadened XRD lines probably do not result from the presence of a mixture of alloy particles differing in an overall composition, but rather from the situation where a relatively thin layer of a Pd-richer phase envelops a Co-richer kernel (seen by XRD). Surface enrichment in Pd is rationalized by the alloy segregation theory (22), based on pure element vaporization enthalpies (90 kcal/mol for Pd, 102.4 kcal/mol for Co). Recent results of Dees and Ponec on 5 wt% Pt–Co/SiO_2 catalysts (*23*) are in harmony with our data. In their X-ray diffractograms, some cobalt was "invisible," as the XRD reflexions were shifted towards positions characteristic of Pt-richer phases. Although Dees and Ponec offer various explanations for their result (*23*), surface enrichment, in this case in cobalt, would rationalize it (vaporization enthalpy for Pt = 135 kcal/mol (*22*)). As the metal loading, type of support, preparation and pretreatment methods employed by Dees and Ponec (*23*) are similar to ours, we feel that the results are complementary. We do not consider a possibility that Co in Pt–Co/SiO_2 forms an unalloyed, silica-bonded XRD-amorphous layer, since Co was easily detected by XRD in Pd–Co/SiO_2.

XPS study confirmed the possibility that Pd segregates to the surface of alloy particles in 10 wt% Pd–Co/SiO_2 (Table 2).

For 1 wt% Pd–Co/SiO_2 catalysts, the XRD analysis is less clear because of a rather low value of the signal-to-noise ratio. XRD peaks were not well resolved and only Pd(111) peaks were well recognized (Table 1). This again may indicate that for this series of Pd–Co samples interaction between

Pd and Co is less strong than in the case of 10 wt% metal-loaded alloys.

Neopentane Conversion

a. Catalytic activity. Tables 3 and 4 show the catalytic results for 1 and 10 wt% Pd–Co/SiO_2, respectively. For better presentation, activity changes with Pd–Co alloy composition at 240°C are shown in Fig. 4: the rates of neopentane conversion pass through distinct minima. We also include a result for a 1 : 1 physical mixture of 10 wt% Pd/SiO_2 with 10 wt% Co/SiO_2 (filled square). It is not surprising that the activity of this physical mixture is much higher than that of Pd50Co50/SiO_2. First, the activities of the physical mixture of both alloy components match (within experimental error) respective curves representing hypothetical activities of physical mixtures of the two components. Second, the fact that activities of bimetallic Pd–Co/SiO_2 catalysts so strongly "deviate" from an additivity, may be regarded as an important result of this work: *neopentane conversion may conveniently be used for probing surfaces of supported Pd–Co.*

In the case of 1 wt%-loaded catalysts, Fig. 4 shows that experimental points for Pd-rich samples do not differ much from those for the 10 wt%-loaded series. This may suggest that homogeneity of Pd-rich catalysts in the 1 wt%-loaded series was good. However, large differences are seen for the Co-rich branch. In the low-loaded series, Co and Co-rich bimetallics are considerably more active than their 10 wt% counterparts. For pure cobalt, the ratio of $TOF_{1\%}$-to-$TOF_{10\%}$ is ca. 20. We presume that this is due to overestimation of $TOF_{1\%Co}$ caused by underestimation of cobalt dispersion. Reuel and Bartholomew (*13*) report that hydrogen chemisorption only partly titrates cobalt in low-loaded Co/support systems. We think that this is due to incomplete reduction, as our TPR studies substantiate such a conclusion. One must, however, assume that unreduced Co species exhibit similar activity to the reduced ones.

b. Isomerization and fragmentation selectivity. Still more remarkable changes with Pd-Co alloy composition are seen for isomerization selectivity (Fig. 5). The Co100/SiO_2 sample exhibits no isomerization (pure cracking), whereas Pd–Co samples show a maximum for intermediate alloy composition. Figure 5a compares isomerization selectivities at 240°C, for 1, 10 wt% Pd–Co/SiO_2, and the 1 : 1 physical mixture of 10 wt% metal-loaded monometallic catalysts. For the 10 wt% metal series, all three bimetallic samples exhibit higher isomerization selectivity than Pd100. On the other hand, for the 1 wt% series, isomerization selectivity of bimetallic samples is comparable to that of Pd100. This fact is in line with our intention: the 1 wt% alloy series was intentionally "poorly" prepared. Relatively high isomerization selectivities for Pd-richer 1 wt% Pd–Co/SiO_2 catalysts can be explained by higher contribution of palladium owing to higher metal dispersion (compared to cobalt, see Table 1). However, it should be stressed here that for Co-richer alloys, the 10 wt%-loaded samples show a higher selectivity increase (compared to pure Pd) than the 1 wt% ones. This could be due to better interaction of the two alloy components in the high-loaded samples and, also, to some surface enrichment in palladium. Again, the experimental point for the physical mixture of the Pd and Co catalysts is far from the respective level of selectivity for well-mixed Pd–Co alloys.

Figure 5 also presents a hypothetical selectivity curve for physical mixtures of 10 wt% Pd/SiO_2 and 10 wt% Co/SiO_2. It is seen that isomerization selectivity for Pd–Co bimetallics follows the order: 10 wt% Pd–Co/SiO_2 > hypothetical physical mixture of 10 wt% Pd/SiO_2 + 10 wt% Co/SiO_2 > experimental value for the 1 : 1 physical mixture of 10 wt% Pd/SiO_2 + 10 wt% Co/SiO_2. While the first part of this sequence is explained by a synergistic effect due to alloying, the second part needs some clarification. We think that such low isomerization selectivity found in the experiment with the

physical mixture is caused by an enhancement in hydrogenolysis at the expense of isomerization. Isopentane (a product of isomerization) is much more reactive on metal surfaces than its parent, especially when hydrogenolysis is expected. Hence a secondary hydrogenolysis of isopentane on contiguous sites of Co causes this large drop in isomerization. Thus the differences in isomerization selectivity between well and poorly mixed Pd–Co alloys should be understood as a result of two effects: synergy in primary isomerization and reduction in secondary hydrogenolysis (due to an absence of contiguous Co sites in well-homogenized alloys).

While Co has no isomerization properties, it is active in hydrogenolysis. That is why evaluation of the alloys produces different results on the basis of the fragmentation factor, ζ. The value of ζ over Co catalyst increases rapidly up to 5 with increasing overall conversion whereas it remained around 2 in a broad range of conversion over Pd (*24*). The values shown in Fig. 6 indicate a predominantly "single hydrogenolysis" in a rather broad range of alloy composition (most molecules broken up produce two fragments only) and this points to a Pd-like behavior of both the 10 and 1 wt% series. These conclusions confirm those already drawn from the isomerization properties.

To sum up, both physical characterization results and Pd-like catalytic characteristics point to a surface enrichment of Pd in the whole range; however, Co exerts a special influence on catalytic properties. Neopentane reactions (isomerization and hydrogenolysis) can offer a convenient basis for probing the surfaces of supported Pd–Co alloys, even though the reason for the synergistic effect for isomerization selectivity on Pd–Co alloys is not clear (an electronic effect has been invoked to interpret the results of hexane conversion over Pt-Co/Al_2O_3 (*25*)). As a matter of fact, such probing has recently been reported; in the case of Pd–Co/NaY, neopentane conversion appears to be a convenient catalytic probe for characterizing interaction between the two metals in the zeolite Y matrix (*26*).

ACKNOWLEDGMENTS

We are indebted to Dr. J. Zieliński for allowing us to use his reactor for carrying out the XRD measurements. XPS analyses were performed by one of us (A.Yu.S.) at the Center for Catalysis and Surface Science, Northwestern University, Evanston, Illinois. We thank Professor Wolfgang Sachtler for advice and helpful discussion and for according us laboratory facilities.

REFERENCES

1. Bond, G. C., *Chem. Soc. Rev.* **20,** 441 (1991).
2. Juszczyk, W., Karpiński, Z., Pielaszek, J., Ratajczykowa, I., and Stanasiuk, Z., *in* "Proceedings, 9th International Congress on Catalysis, Calgary, 1988" (M. J. Phillips and M. Ternan, Eds.), Vol. 3, p. 1238. Chem. Institute of Canada, Ottawa, 1988.
3. Juszczyk, W., and Karpiński, Z., *J. Catal.* **117,** 519 (1989).
4. Juszczyk, W., Karpiński, Z., Ratajczykowa, I., Stanasiuk, Z., Zieliński, J., Sheu, L.-L., and Sachtler, W. M. H., *J. Catal.* **120,** 68 (1989).
5. Matsumoto, H., Saito, Y., and Yoneda, Y., *J. Catal.* **22,** 182 (1971).
6. Boudart, M., and Ptak, L. D., *J. Catal.* **16,** 90 (1970).
7. Anderson, J. R., and Avery, N. R., *J. Catal.* **5,** 446 (1966).
8. E.g., Anderson, J. R., and Mainwaring, D. E., *J. Catal.* **35,** 162 (1974).
9. Margitfalvi, J., Gobolos, S., Hegedus, M., Tálas, E., *in* "Proceedings 8th International Congress on Catalysis, Berlin, 1984", Vol. IV, p. 903. Verlag Chemie, Weinheim, 1984.
10. Juszczyk, W., Karpiński, Z., Paál, Z., and Pielaszek, J., *in* "Proceedings, 10th International Congress on Catalysis, Budapest, 1992" (L. Guczi, F. Solymosi, and P. Tétényi, Eds.), Part B, p. 1843. Akadémiai Kiadó/Elsevier, Budapest/Amsterdam, 1993.
11. Juszczyk, W., Karpiński, Z., Pielaszek, J., and Paál, Z., in press.
12. Aben, P. C., *J. Catal.* **10,** 224 (1968).
13. Reuel, R. C., and Bartholomew, C. H., *J. Catal.* **85,** 63 (1984).
14. Zieliński, J., and Borodziński, A., *Appl. Catal.* **13,** 305 (1985).
15. Pielaszek, J., *in* "Advanced Methods in X-Ray and Neutron Structure Analysis of Materials" (J. Hasek, Ed.), p. 209. Plenum, New York, 1989.
16. Pielaszek, J., *Z. Kristallogr.* **185,** 703 (1988).
17. Wagner, C. D., Davis, L. E., Zeller, M. V., Taylor,

J. A., Raymond, R. H., and Gale, L. H., *Surf. Interface Anal.* **3,** 211 (1981).
18. Shamsuddin, M., and Kleppa, O. J., *J. Chem. Phys.* **80,** 3760 (1984).
19. Ichikawa, S., Poppa, H., and Boudart, M., *J. Catal.* **91,** 1 (1985).
20. Paál, Z., and Tétényi, P., *Nature* **267,** 234 (1977).
21. Paryjczak, T., Rynkowski, J., and Karski, S., *J. Chromatogr.* **188,** 254 (1980).
22. Williams, F. L., and Nason, D., *Surf. Sci.* **45,** 377 (1974).
23. Dees, M. J., and Ponec, V., *J. Catal.* **119,** 376 (1989).
24. Paál, Z., Tétényi, P., and Dobrovolszky, M., *React. Kinet. Catal. Lett.* **37,** 163 (1988).
25. Zyade, S., Garin, F., and Maire, G., *New J. Chem.* **11,** 429 (1987).
26. Karpiński, Z., Zhang, Z., and Sachtler, W. M. H., *Catal. Lett.* **13,** 123 (1992).